THE JOURNAL OF BIOLOGICAL CHEMISTRY
Vol. 278, No. 19, Issue of May 9, pp. 17108–17113, 2003
Printed in U.S.A.

An Ile-568 to Asn Polymorphism Prevents Normal Trafficking and Function of the Human $P2X_7$ Receptor*

Received for publication, December 16, 2002, and in revised form, February 12, 2003
Published, JBC Papers in Press, February 13, 2003, DOI 10.1074/jbc.M212759200

James S. Wiley‡§, Lan-Phuong Dao-Ung‡, Changping Li‡, Anne N. Shemon‡, Ben J. Gu‡, Megan L. Smart¶, Stephen J. Fuller‡, Julian A. Barden‖, Steven Petrou¶, and Ronald Sluyter‡

From the ‡Department of Medicine, University of Sydney at Nepean Hospital, Penrith, New South Wales 2750, the ¶Department of Physiology, University of Melbourne, Parkville, Victoria 3050, and the ‖Department of Anatomy and Histology, University of Sydney, Sydney, New South Wales 2006, Australia

The $P2X_7$ receptor is a ligand-gated channel that is highly expressed on mononuclear cells and that mediates ATP-induced apoptosis of these cells. Wide variations in the function of the $P2X_7$ receptor have been observed, in part because of a loss-of-function polymorphism that changes Glu-496 to Ala without affecting the surface expression of the receptor on lymphocytes. In this study a second polymorphism (Ile-568 to Asn) has been found in heterozygous dosage in three of 85 normal subjects and in three of 45 patients with chronic lymphocytic leukemia. $P2X_7$ function was measured by ATP-induced fluxes of Rb^+, Ba^{2+}, and ethidium$^+$ into various lymphocyte subsets and was decreased to values of ~25% of normal. The expression of the $P2X_7$ receptor on lymphocytes was approximately half that of normal values as measured by the binding of fluorescein-conjugated monoclonal antibody. Transfection experiments showed that $P2X_7$ carrying the Ile-568 to Asn mutation was non-functional because of the failure of cell surface expression. The differentiation of monocytes to macrophages with interferon-γ up-regulated $P2X_7$ function in cells heterozygous for the Ile-568 to Asn mutation to a value around 50% of normal. These data identify a second loss-of-function polymorphism within the $P2X_7$ receptor and show that Ile-568 is critical to the trafficking domain, which we have shown to lie between residues 551 and 581.

The purinergic $P2X_7$ receptor is a ligand-gated channel, selective for cationic permeants, which has a wide distribution including cells of the immune and hemopoietic system (1, 2). Activation of this receptor by brief exposure to extracellular ATP opens a channel that allows Ca^{2+} and Na^+ influx and K^+ efflux and that initiates a cascade of intracellular downstream events. These include the stimulation of phospholipase D (3, 4), the activation of membrane metalloproteases (5–7), and the stimulation of intracellular caspases, which eventually lead to the apoptotic death of the target cell (8, 9). $P2X_7$ activation also leads to extensive membrane blebbing (10), which is a typical morphological feature of the apoptotic process. $P2X_7$ receptors have two transmembrane domains with intracellular amino and carboxyl termini, and the $P2X_7$ receptor differs from other members of the P2X receptor family in having a long carboxyl terminus of 240 amino acids from the inner membrane face (11). This long carboxyl terminus is necessary for the permeability properties of the $P2X_7$ receptor because truncation of this tail abolishes ATP-induced uptake of the fluorescent dye Yo-Pro-1 (12). $P2X_7$ has an oligomeric structure in the membrane based on trimeric or larger complexes of identical subunits (13, 14), and there is evidence that $P2X_7$ interacts with a number of structural and adhesion proteins in a complex at the cell surface (15). Phosphorylation of a tyrosine at amino acid 343 of the $P2X_7$ primary structure has been proposed as being important for maintaining the full activity of the $P2X_7$ channel (15).

A number of regulatory domains or motifs have been identified in the intracellular carboxyl tail based on homology with other proteins. These include a potential Src homology 3 binding domain (amino acids 450–456) and an ankyrin repeat motif (amino acids 494–508) (16). Ankyrin repeats have been shown to play a major structural role in protein anchoring to the membrane or cytoskeleton, protein folding, and protein-protein interaction (17, 18). In addition, a lipopolysaccharide (LPS)[1] binding motif with homology to the LPS-binding protein of plasma (16) has been proposed between amino acids 573 and 590, whereas we have shown that a region within this motif (amino acids 551–581) is necessary for the surface expression of $P2X_7$ (19). Upstream from this motif we have identified a single nucleotide polymorphism (1513A→C), present in around 20% of the population, which changes Glu to Ala at amino acid 496 and which leads to loss of function of the receptor (20). Surface expression of $P2X_7$ on lymphocytes was not affected by the Glu-496 to Ala polymorphism, suggesting that the loss of function resulted from impaired protein-protein interactions in the $P2X_7$ complex at the cell membrane rather than from trafficking to the surface (20). In this study, we report the functional effects of a second polymorphism of the human *P2X7* gene (thymine to adenine at position 1729 of cDNA) that is associated with loss of function of the $P2X_7$ receptor because of failure of its trafficking to the cell surface. This polymorphism changes Ile to Asn at amino acid 568, which localizes this residue as being within a trafficking motif in the carboxyl tail of the receptor.

EXPERIMENTAL PROCEDURES

Materials—ATP, ethidium bromide, $BaCl_2$, D-glucose, bovine serum albumin, RPMI 1640 medium, gentamicin, collagen (Type X), and glyc-

* This work was supported by the National Health and Medical Research Council, the Cure Cancer Australia Foundation, and the Leukaemia Foundation of Australia. The costs of publication of this article were defrayed in part by the payment of page charges. This article must therefore be hereby marked "*advertisement*" in accordance with 18 U.S.C. Section 1734 solely to indicate this fact.

§ To whom correspondence should be addressed: Level 5, South Block, Nepean Hospital, Penrith, NSW 2750, Australia. Tel.: 61-2-4734-3277; Fax: 61-2-4734-3432; E-mail: wileyj@medicine.usyd.edu.au.

[1] The abbreviations used are: LPS, lipopolysaccharide; CLL, chronic lymphocytic leukemia; FITC, fluorescein isothiocyanate; mAb, monoclonal antibody(ies); HEK, human embryonic kidney; NK, natural killer.

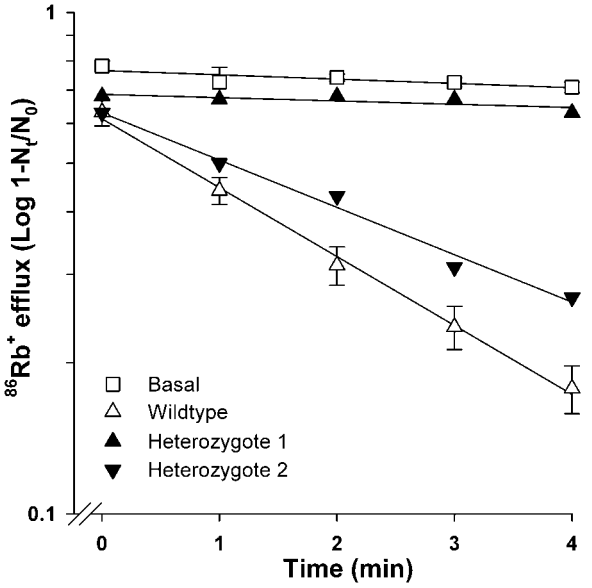

FIG. 1. **ATP-induced Rb^+ efflux from lymphocytes from CLL subjects either wild type or heterozygous for the 1729A allele.** Lymphocytes from CLL subjects either wild type at 1729 (△) or heterozygous for the 1729A allele (▲, ▼) were loaded for 2 h with $^{86}Rb^+$. Cells were washed, resuspended in KCl medium, and incubated for 5 min at 37 °C before incubation with 0.5 mM ATP for 4 min. Samples (1 ml) were collected at 1-min intervals. Basal $^{86}Rb^+$ efflux measured in the absence of ATP is shown (□). $^{86}Rb^+$ efflux is expressed as $(1 - N_t/N_o)$, where N_t is the level of cell-associated radioactivity at time t (determined by Cerenkov counting) and N_o the amount of cell-associated radioactivity at time 0. The data have been analyzed after log transformation to permit calculation of efflux rate constants. Results from seven different subjects wild type at 1729 are shown as the mean ± S.E. Results from two different subjects heterozygous for the 1729A allele are shown as separate *lines* (one *line* being representative of two experiments for each heterozygote subject).

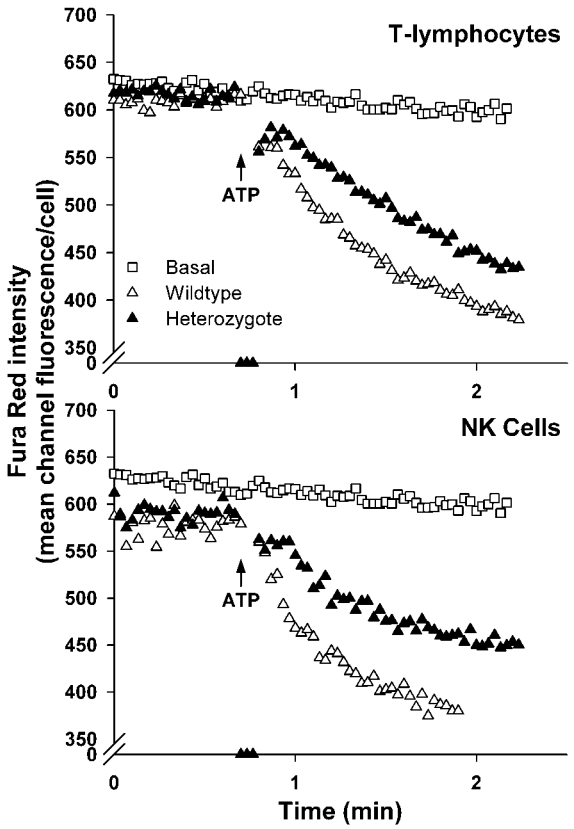

FIG. 2. **ATP-induced Ba^{2+} influx into normal human T-lymphocytes and NK cells from subjects either wild type or heterozygous for the 1729A allele.** Mononuclear cells from normal subjects either wild type at 1729 (△) or heterozygous for the 1729A allele (▲) were incubated with 1 μg/ml Fura Red for 30 min and washed once. The cells were labeled with FITC-conjugated anti-CD3 or -CD16 mAb and resuspended in KCl medium at 37 °C. Ba^{2+} (1 mM) was added and was followed 40 s later by the addition of 1 mM ATP (*arrow*). The mean channel of cell-associated fluorescence intensity was measured at 2-s intervals for gated $CD3^+$ T-lymphocytes (*top panel*) or $CD16^+$ NK cells (*bottom panel*). Basal Ba^+ influx measured in the absence of ATP is shown (□). The arbitrary units of the area above the Ba^{2+} influx curve in the first 20 s after the addition of ATP are 1519 for wild type T-lymphocytes, 720 for heterozygous T-lymphocytes, 2265 for wild type NK cells, and 1038 for heterozygous NK cells. The figure depicts one representative experiment of three performed.

erol gelatin mounting medium were purchased from Sigma. Interferon-γ was obtained from Roche Diagnostics. HEPES, fetal calf serum, normal horse serum, LipofectAMINE™ 2000 reagent, Opti-MEM I medium, and *Taq* DNA polymerase were purchased from Invitrogen. Ficoll-Paque™ and $^{86}RbCl$ (1.5 mCi/ml; specific radioactivity, 3 Ci/mmol) were purchased from Amersham Biosciences. Di-*n*-butyl phthalate and di-isooctyl phthalate (Merck Chemicals Ltd., Poole, England) were blended 80:20 (v/v) to give a mixture of density 1.030 g/ml. Fura Red™, AM was obtained from Molecular Probes. Fluorescein isothiocyanate (FITC)- and phycoerythrin-conjugated anti-CD monoclonal antibodies (mAb) were acquired from Dako. Cy3-conjugated donkey anti-sheep IgG antibody was purchased from Jackson ImmunoResearch. Murine anti-human $P2X_7$ receptor mAb (kindly provided by Drs. Gary Buell and Ian Chessell) (21) was purified from clone L4 hybridoma supernatant by chromatography on protein A-Sepharose fast flow and conjugated to FITC as described (22). Sheep polyclonal anti-$P2X_7$ antibody against a non-homologous extracellular epitope of the human $P2X_7$ receptor (23) was produced as described for a sheep polyclonal anti-$P2Y_1$ antibody (24). Specificity of the polyclonal anti-$P2X_7$ antibody was confirmed by binding to human embryonic kidney (HEK)-293 cells transfected with human $P2X_7$ cDNA but not to mock-transfected or non-transfected HEK-293 cells (Fig. 5 and results not shown). Preimmune serum failed to bind transfected, mock-transfected, or non-transfected HEK-293 cells (results not shown).

Source of Human Leukocytes—Peripheral blood mononuclear cells were isolated by density gradient centrifugation as described (22). Cells were resuspended in HEPES-buffered NaCl medium (145 mM NaCl, 5 mM KCl, 10 mM HEPES, 5 mM D-glucose, and 1 mg/ml bovine serum albumin, pH 7.5) containing 1 mM $CaCl_2$ or RPMI 1640 medium containing 10% fetal calf serum and 5 μg/ml gentamicin (complete medium). For the generation of macrophages, the mononuclear cell preparation in complete medium was incubated for 2 h in plastic flasks and then gently washed to remove non-adherent cells. The plastic-adherent monocytes were differentiated into macrophages by culturing for 7 days in complete medium. Macrophages were activated by adding 100 units/ml interferon-γ in the final 24 h of culture before harvesting by mechanical scraping for flow cytometric analysis.

$^{86}Rb^+$ Efflux Measurements—ATP-induced $^{86}Rb^+$ efflux from chronic lymphocytic leukemia (CLL) lymphocytes was performed as described (25).

Ba^{2+} Influx Measurements—Mononuclear cells (4×10^6) were incubated with Fura Red (1 μg/ml) for 30 min at 37 °C in HEPES-buffered NaCl medium. Cells then were washed once and labeled with appropriate FITC-conjugated anti-CD mAb for 15 min. Cells were washed once and resuspended in 1.0 ml of HEPES-buffered KCl medium (150 mM KCl, 10 mM HEPES, 5 mM D-glucose, 0.1% bovine serum albumin, pH 7.5) at 37 °C. All samples were stirred and maintained at 37 °C using a Time Zero module (Cytek, Fremont, CA). $BaCl_2$ (1.0 mM) was added and was followed 40 s later by the addition of 1.0 mM ATP. Cells were analyzed at 2000 events/s on a FACSCalibur flow cytometer (BD Biosciences) and were gated by forward and side scatter and by cell type-specific antibodies. The linear mean channel of fluorescence intensity (0–1023 channel) for each gated subpopulation over successive 2-s intervals was analyzed by WinMDI software (Joseph Trotter, version 2.7) and plotted against time.

Ethidium$^+$ Influx Measurements—ATP-induced ethidium$^+$ influx into mononuclear cells from normal and CLL subjects and into HEK-293 cells was performed using time-resolved flow cytometry as described (22). Because of the increased $P2X_7$ function on macrophages, data for comparison of ethidium$^+$ uptake between monocytes and macrophages (Fig. 6) were acquired at a reduced voltage setting for FL-2 (ethidium$^+$ fluorescence) as described (7).

TABLE I
Reduced P2X$_7$ expression and function in leukocytes with the 1729A allele

	Genotype		P2X$_7$ expression (mean channels of fluorescence intensity)		P2X$_7$ function (arbitrary units of area under ATP-induced ethidium$^+$ uptake curve at 5 min)		
	1513	1729	T-lymphocyte	B-lymphocyte	T-lymphocyte	B-lymphocyte	Monocyte
Normal subjects							
N1	A/A	T/A	2.6	3.9	265	683	4592
N2	A/A	T/A	3.5	5.1	219	194	440
N3	A/A	T/A	2.1	5.5	553	719	10,281
B-CLL subjects							
CLL1	A/A	T/A	1.7	4.1	68	70	0
CLL2	A/A	T/A			60	948	546
Normal subjects[a]	A/A	T/T	7.7 ± 1.2	9.6 ± 1.3	3115 ± 722	3569 ± 662	19,371 ± 2244

[a] Mean ± S.E., n = 14–16.

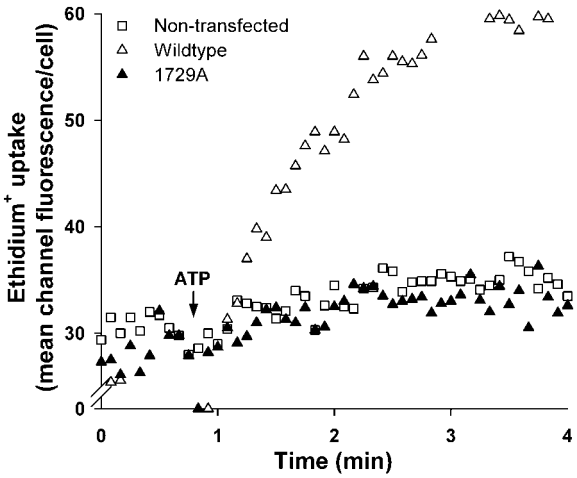

FIG. 3. **ATP-induced ethidium$^+$ uptake into HEK-293 cells transfected with wild type or 1729A-mutated P2X$_7$ cDNA.** HEK-293 cells transiently transfected either with wild type (△) or 1729A-mutated P2X$_7$ cDNA (▲) or with non-transfected HEK-293 cells (□) were washed and resuspended in 1 ml of KCl medium. Ethidium$^+$ (25 μM) was added and was followed 40 s later by the addition of 1 mM ATP (*arrow*). The mean channel of cell-associated fluorescence intensity was measured at 5-s intervals for gated HEK-293 cells. The figure depicts one representative experiment of three performed.

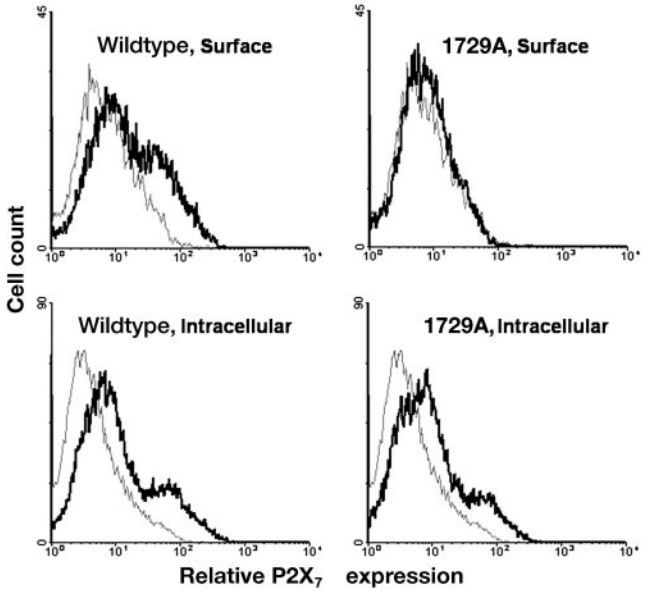

FIG. 4. **Flow cytometric histograms of wild type and 1729A-mutated P2X$_7$ expression in HEK-293 cells.** HEK-293 cells were transiently transfected with either wild type (*left panels*) or 1729A-mutated (*right panels*) P2X$_7$ cDNA. Non-permeabilized cells (*top panels*, surface P2X$_7$ expression) and fixed and permeabilized cells (*bottom panels*, intracellular P2X$_7$ expression) were labeled with FITC-conjugated anti-P2X$_7$ mAb (*black line*) or isotype control mAb (*shaded line*), and the level of P2X$_7$ expression was determined by flow cytometry. The figure depicts one representative experiment of three performed.

DNA Extraction, Polymerase Chain Reaction, and DNA Sequencing—Genomic DNA was extracted from peripheral blood using the Wizard genomic DNA purification kit (Promega) according to the manufacturer's instructions. A primer pair was designed within exon 13 of the *P2X7* gene to amplify a 579-bp product from genomic DNA. P2X$_7$ oligonucleotides were synthesized by Invitrogen. The forward primer was 5′-GAACCTAGAACCTGAGGGCT-3′, and the reverse primer was 5′-CAGACGTGAGCCACGGTGC-3′. PCR amplification (32 cycles of denaturation at 95 °C for 45 s, annealing at 56 °C for 45 s, and extension at 72 °C for 1 min) produced a fragment of the expected 579-bp size. Amplified PCR products were purified (GFX™ PCR DNA and gel band purification kit, Amersham Biosciences) and sequenced as described (20).

Site-directed Mutagenesis—Mutated 1729T→A was introduced using overlap PCR (QuikChange™ site-directed mutagenesis kit, Stratagene) and the expression vector pCI-hP2X$_7$ as described (20). The primer sequences were as follows (base changes are in bold and underlined): T1729A forward, C ATG GCT GAC TTT GCC A**A**C CTG CCC AGC TGC TGC C; T1729A reverse, G GCA GCA GCT GGG CAG G**T**T GGC AAA GTC AGC CAT G.

Transfection of HEK-293 Cells—HEK-293 cells were transfected with P2X$_7$ cDNA using LipofectAMINE™ 2000 reagent diluted in Opti-MEM I medium as described (20). Cells were collected after 40–44 h by mechanical scraping.

Immunofluorescent Staining and Flow Cytometry—Surface and intracellular P2X$_7$ receptor expression on mononuclear cells and on HEK-293 cells was measured by multicolor flow cytometry as described previously (22).

Immunofluorescent Staining and Confocal Microscopy—HEK-293 cells incubated on collagen-coated coverslips were fixed (2% paraformaldehyde), and P2X$_7$ receptor expression was determined using immunocytochemistry and confocal microscopy as described (26). For intracellular staining, cells were permeabilized with 0.1% Triton X-100, 0.1% dimethyl sulfoxide, and 2% normal horse serum in phosphate-buffered saline for 10 min and washed three times with phosphate-buffered saline before immunolabeling.

RESULTS

A Single Nucleotide Polymorphism at Position 1729 of the P2X7 Gene—A PCR product was amplified directly from genomic DNA to include the whole of exon 13 of the *P2X7* gene, and the product was sequenced. In three of 85 normal subjects, a heterozygous nucleotide substitution (thymine to adenine) was found at position 1729, but no homozygous substitutions were observed. The overall allele frequency of this single nucleotide polymorphism (1729T→A) was 0.04 in the Caucasian population. A comparable allele frequency of 0.06 was found in 45 patients with CLL of whom three were heterozygous for the 1729A allele. The deduced amino acid change for this polymorphism is isoleucine to asparagine at amino acid 568 (I568N) of the P2X$_7$ protein. All six subjects who were heterozygous for 1729T→A were wild type for the polymorphism that we have described previously at nucleotide 1513 of the *P2X7* gene (20). Subjects identified previously as homozygous for the loss-of-function 1513A→C polymorphism (20) were wild type at position 1729.

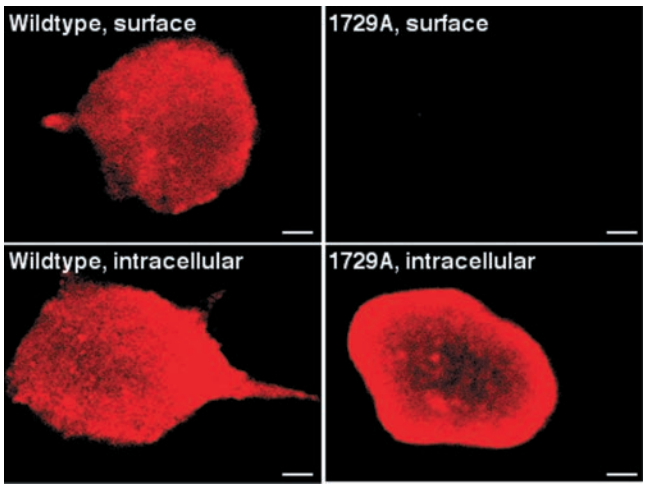

FIG. 5. **Confocal microscope images of wild type and 1729A-mutated $P2X_7$ expression in HEK-293 cells.** HEK-293 cells were transiently transfected with either wild type (*left panels*) or 1729A-mutated (*right panels*) $P2X_7$ cDNA. Non-permeabilized (*top panels*, surface $P2X_7$ expression) or permeabilized (*bottom panels*, intracellular $P2X_7$ expression) cells were incubated with anti-$P2X_7$ antibody and subsequently with Cy3-conjugated anti-sheep IgG antibody before analysis by confocal microscopy. The *calibration bar* is 2 μm.

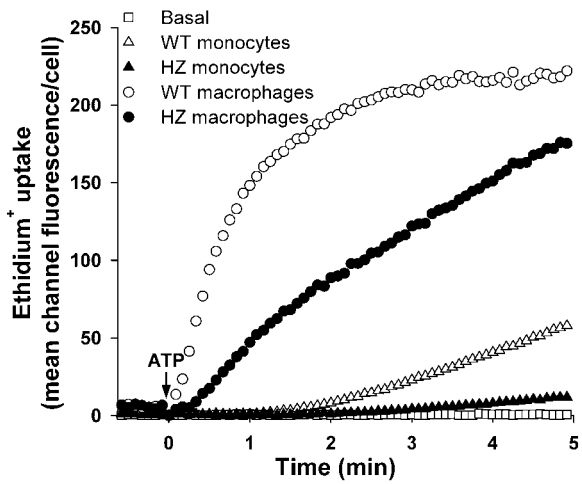

FIG. 6. **ATP-induced ethidium$^+$ uptake in monocytes and monocyte-derived macrophages from normal subjects either wild type or heterozygous at position 1729 of the *P2X7* gene.** Fresh monocytes (△, ▲) or 7-day monocyte-derived macrophages (activated with interferon-γ) (○, ●) from subjects either wild type at 1729 (△, ○) or heterozygous for the 1729A allele (▲, ●) were labeled with FITC-conjugated anti-CD14 mAb and suspended in KCl medium at 37 °C. Ethidium$^+$ (25 μM) was added and was followed 40 s later by the addition of 1 mM ATP (*arrow*). The mean channel of cell-associated fluorescence was measured by time-resolved flow cytometry. Basal ethidium$^+$ uptake measured in the absence of ATP is shown (□). The figure depicts one representative experiment of two performed.

ATP-induced ^{86}Rb Efflux from Lymphocytes—The function of the $P2X_7$ channel was measured by the ATP-induced efflux of isotopic Rb^+ from lymphocytes (>98% purity) from the peripheral blood of subjects with CLL (25). The lymphocytes were loaded with $^{86}Rb^+$ in a 2-h preincubation, washed, and incubated at 37 °C with or without the addition of 1 mM ATP. In lymphocytes that were wild type for both 1729T and 1513A alleles, the loss of $^{86}Rb^+$ from the cells over 4 min followed first-order kinetics with a rate constant of 0.03 ± 0.01 min^{-1} (range of 0.01–0.05, $n = 7$) in the absence of ATP and 0.34 ± 0.04 min^{-1} (range of 0.24–0.50, $n = 7$) in the presence of ATP (Fig. 1). In two subjects heterozygous for the 1729A allele, the function of the lymphocyte $P2X_7$ channel was either absent or reduced (Fig. 1). In one heterozygote the rate constant for $^{86}Rb^+$ efflux from lymphocytes was the same in the absence and presence of ATP (0.02 and 0.03 min^{-1}, respectively), whereas in the other heterozygote the addition of ATP increased the rate constant from 0.02 to 0.23 min^{-1}. Data from duplicate experiments for each heterozygote provided in the presence of ATP a mean rate constant of 0.12 ± 0.07 min^{-1} ($n = 4$), which was significantly lower than the rate constant of 0.34 ± 0.04 min^{-1} ($n = 7$) for wild type lymphocytes ($p < 0.01$, Mann-Whitney U test). Measurement of isotopic Rb^+ efflux from lymphocytes of normal subjects was complicated by the variable admixture of monocytes with lymphocytes, and we turned to flow cytometric methods to study $P2X_7$ channel fluxes in defined leukocyte subsets.

$P2X_7$ Expression and Function in Lymphocytes and Monocytes—The permeability of the $P2X_7$ channel was studied by two-color flow cytometry in which the influx of Ba^{2+} was measured into lymphocytes (either T-lymphocyte or NK cell subsets) identified by appropriate FITC-conjugated mAb. Fig. 2 shows the ATP-induced uptake of Ba^{2+} into lymphocytes from a normal subject loaded with Fura Red for which fluorescence emission measured by flow cytometry decreases upon the entry of Ba^{2+} into the cell. The rate of Ba^{2+} uptake into lymphocytes from this normal subject heterozygous for the 1729A allele was markedly decreased compared with a normal subject who was wild type at this position (Fig. 2). Similar results were observed for the two CLL subjects heterozygous for the 1729A allele (data not shown). A more quantitative estimate of $P2X_7$ receptor channel function was obtained by ATP-induced uptake of a larger permeant, the fluorescent cation ethidium$^+$, for which uptake into lymphocyte and monocyte subsets was measured by time-resolved two-color flow cytometry (22). In three normal subjects who were heterozygous for 1729A, the ATP-induced ethidium$^+$ uptakes were extremely low (only 11–26% of normal mean values (Table I)). The magnitude of the reduction was similar and significant for the three normal cell types studied (T-lymphocytes, $p < 0.05$; B-lymphocytes, $p < 0.01$; monocytes, $p < 0.02$; Mann-Whitney U test). Surface expression of the $P2X_7$ receptor was measured by the binding of a FITC-conjugated mAb against the extracellular domain of $P2X_7$ (21). $P2X_7$ expression in the three normal subjects heterozygous for the 1729A allele averaged 35 and 50% of the normal mean expression on T- and B-lymphocytes, respectively. Similar results were obtained for lymphocytes and monocytes from two of the subjects with CLL who were heterozygous for the 1729A allele. Both had very low or absent $P2X_7$ function in T-lymphocyte, B-lymphocyte, and monocyte subsets, whereas the surface expression of $P2X_7$ in one heterozygous CLL subject was less than half of the mean value for wild type cells from normal subjects (Table I).

Expression and Function of Ile-568 to Asn-mutated $P2X_7$—cDNA for wild type $P2X_7$ or $P2X_7$ carrying the 1729T→A mutation was transfected into HEK-293 cells, and the expression and function of the receptor were measured. At 40 h after transfection, strong surface expression and function of wild type $P2X_7$ were observed, but the 1729T→A-mutated $P2X_7$ was non-functional using the ATP-induced ethidium$^+$ uptake assay (Fig. 3). The basis for the loss of $P2X_7$ function was failure of trafficking of the mutant receptor to the cell surface shown by the absence of surface $P2X_7$ immunoreactivity in cells transfected with mutated $P2X_7$ and incubated with a mAb to the extracellular domain of $P2X_7$ (Fig. 4). Confocal microscopy confirmed the absence of surface expression of 1729T→A-mutated $P2X_7$, although strong intracellular staining for mutated $P2X_7$ was seen in permeabilized cells (Fig. 5).

Macrophage $P2X_7$ Function—Differentiation of monocytes

into macrophages increases the expression and function of P2X$_7$ by manyfold (27). Peripheral blood monocytes were cultured for 7 days (with interferon-γ present for the final 24 h), and the P2X$_7$ function was measured by ATP-induced ethidium$^+$ uptake into the CD14$^+$ macrophage population. Macrophages from a normal subject with wild type P2X$_7$ had an ATP-induced ethidium$^+$ uptake 10-fold greater than their precursor monocytes (Fig. 6). Thus the area under the ATP-induced ethidium$^+$ uptake curve increased from 5193 units on day 0 monocytes to 49,314 units on day 7 macrophages. Macrophages from a normal subject heterozygous for the 1729A allele also increased their P2X$_7$ function from 845 units on day 0 monocytes to 26,606 on day 7 macrophages, but this function was only 54% that of macrophages that were wild type with both 1729T and 1513A alleles (Fig. 6).

DISCUSSION

The present study has identified a single nucleotide polymorphism that leads to a loss of function of P2X$_7$ because of a trafficking defect in this receptor. This polymorphism was at position 1729T→A of the cDNA that changes isoleucine to asparagine at amino acid position 568. Three of 85 normal subjects were found to be heterozygous for this polymorphic variation, and all three had half-normal expression of the P2X$_7$ on the cell surface and reduction of P2X$_7$ function to ~25% of normal. Transfection experiments provided confirmation that the Ile-568 to Asn-mutated P2X$_7$ fails to traffic to the cell surface. HEK-293 cells transfected with this mutated P2X$_7$ showed neither surface expression nor function despite plentiful intracellular synthesis of this receptor (Figs. 4 and 5). In other experiments, we measured the physiological properties of the Ile-568 to Asn-mutated P2X$_7$ in *Xenopus* oocytes and found channel currents in oocytes that were identical to those with the wild type P2X$_7$ construct.[2] This result shows that the Ile-568 to Asn mutation does not alter the function of the P2X$_7$ channel, although this result shows differences in trafficking between the mammalian and amphibian expression systems. A number of functional domains have been proposed in the long carboxyl terminus of P2X$_7$ based on protein sequence homology. The most distal of these, the "LPS-binding domain" from amino acids 573 to 590, has homology with the LPS-binding protein of plasma and has been suggested to interact directly with internalized LPS (16). Using a series of truncated mutants of rat P2X$_7$, we have identified previously a region between residues 551 and 581 that is both highly conserved and necessary for the surface expression of this receptor (19). Mutation of the conserved residues at Cys-572, Arg-574, and Phe-581 abolished both cell surface expression and receptor function (19), suggesting that the trafficking domain of P2X$_7$ overlaps the putative LPS-binding domain. The present data add the conserved Ile-568 to the other residues within this trafficking domain required for cell surface expression of P2X$_7$. Whether this domain binds directly to phospholipid or to one of the many protein partners in the P2X$_7$ membrane complex (15) is uncertain. However, this domain includes a conserved cysteine, palmitoylation of which is required for cell surface expression in a number of other receptors such as CCR5 (28). Recently, P2X$_4$ but not P2X$_2$ receptors have been shown to undergo constitutive endocytosis in neurons (29). Whether P2X$_7$ also undergoes constitutive endocytosis is unknown, but the lack of 1729T→A-mutated P2X$_7$ expressed on the surface of HEK-293 cells may be because of the rapid endocytosis of the receptor after initial trafficking to the cell surface. This, however, seems unlikely, as we failed to detect mutant P2X$_7$ on the surface of HEK-293 cells using either flow cytometry or confocal microscopy.

Wide variations in the function of the P2X$_7$ receptor have been observed in lymphocytes both from normal subjects (20) and patients with CLL (30). Some but not all of this variability is a result of a single nucleotide polymorphism (1513A→C) that changes Glu-496 to Ala and leads to loss of function without affecting surface expression of the receptor in lymphocytes (20). The trafficking-defective polymorphism identified in the present study, Ile-568 to Asn, contributes to this variability in P2X$_7$ function but with a lower heterozygote prevalence of ~4% compared with ~20% for the more common Glu-496 to Ala variation. Collectively, however, these two genotypes still do not account for all individuals with low or absent P2X$_7$ function (20, 30). The coding region within exon 13 of the *P2X7* gene is highly polymorphic with five single nucleotide polymorphisms identified within a 0.5-kb stretch of cDNA,[3] and it is likely that other loss-of-function polymorphisms exist in the *P2X7* gene, both within the coding region and in the upstream promoter of this gene (31). Recently a polymorphism affecting the function of the mouse P2X$_7$ receptor has been recognized in inbred strains of mice. Although most strains of mice carried Pro-451 with good P2X$_7$ function, C57BL and DBA strains possessed a Leu-451 allele with lower P2X$_7$ function (32). Whether the recognition or docking sequence around residue 451 lies within a domain interacting with a Src homology 3-binding protein is not known. We have surveyed 99 human base sequences coding for residue 451 but have found no deviations from the wild type sequence.[4]

An increasing number of channelopathies have been associated with human disease. Thus hypokalemic periodic paralysis and familial hemiplegic migraine result from missense or point mutations in a voltage-sensitive calcium channel (33, 34). Mutations in sodium and potassium channels also can cause neurological disease with ataxic or epileptic phenotypes (34–36). There is increasing interest in channelopathies that affect cells of the immune system and the impact of reduced or absent P2X$_7$ channel function on human susceptibility to infectious diseases. P2X$_7$ receptor expression is up-regulated on differentiation of monocytes to macrophages (27), where its activation is necessary both for the ATP-induced killing of ingested mycobacterial species and for the subsequent apoptotic death of this phagocytic cell (37–39). Whether Asn-568 (1729A allele) as well as Ala-496 (1513C allele) contribute to the genetic susceptibility to tuberculous infection is uncertain, although macrophages from subjects heterozygous for Asn-568 failed to up-regulate P2X$_7$ function to the same extent as wild type subjects (Fig. 6). Although a mouse strain of P2X$_7$-null genotype has been developed, there is no distinctive adverse phenotype of this animal (40, 41). However, the severity of inflammatory arthritis induced by anti-collagen antibody was markedly attenuated in these animals (41). It seems likely that the P2X$_7$ receptor and its polymorphic variants will be central in our understanding of certain inflammatory and infectious diseases.

Acknowledgments—We thank Dr. Diane Williams for blood collection; Prof. Graeme Stewart, Dr. David Booth, and Maria Ban for helpful discussions; Shelley Spicer for typing this manuscript; and Kristen Skarratt for critically reviewing the manuscript.

REFERENCES

1. Di Virgilio, F., Chiozzi, P., Ferrari, D., Falzoni, S., Sanz, J. M., Morelli, A., Torboli, M., Bolognesi, G., and Baricordi, O. R. (2001) *Blood* **97,** 587–600
2. North, R. A. (2002) *Physiol. Rev.* **82,** 1013–1067
3. El-Moatassim, C., and Dubyak, G. R. (1993) *J. Biol. Chem.* **268,** 15571–15578
4. Gargett, C. E., Cornish, E. J., and Wiley, J. S. (1996) *Biochem. J.* **313,** 529–535
5. Jamieson, G. P., Snook, M. B., Thurlow, P. J., and Wiley, J. S. (1996) *J. Cell. Physiol.* **166,** 637–642
6. Gu, B., Bendall, L. J., and Wiley, J. S. (1998) *Blood* **92,** 946–951

[2] M. L. Smart, unpublished observations.

[3] C. Li, R. Sluyter, B. J. Gu, and J. S. Wiley, unpublished observations.

[4] C. Li and J. S. Wiley, unpublished observations.

7. Sluyter, R., and Wiley, J. S. (2002) *Int. Immunol.* **14,** 1415–1421
8. Ferrari, D., Los, M., Bauer, M. K. A., Vandenabeele, P., Wesselborg, S., and Schulze-Osthoff, K. (1999) *FEBS Lett.* **447,** 71–75
9. Humphreys, B. D., Rice, J., Kertesy, S. B., and Dubyak, G. R. (2000) *J. Biol. Chem.* **275,** 26792–26798
10. Virginio, C., MacKenzie, A., North, R. A., and Surprenant, A. (1999) *J. Physiol. (Lond.)* **519,** 335–346
11. Rassendren, F., Buell, G., Newbolt, A., North, R. A., and Surprenant, A. (1997) *J. Biol. Chem.* **272,** 5482–5486
12. Surprenant, A., Rassendren, F., Kawashima, E., North, R. A., and Buell, G. (1996) *Science* **272,** 735–738
13. Nicke, A., Baumert, H. G., Rettinger, J., Eichele, A., Lambrecht, G., Mutschler, E., and Schmalzing, G. (1998) *EMBO J.* **17,** 3016–3028
14. Kim, M., Spelta, V., Sim, J., North, R. A., and Surprenant, A. (2001) *J. Biol. Chem.* **276,** 23262–23267
15. Kim, M., Jiang, L.-H., Wilson, H. L., North, R. A., and Surprenant, A. (2001) *EMBO J.* **20,** 6347–6358
16. Denlinger, L. C., Fisette, L., Sommer, J. A., Watters, J. J., Prabhu, U., Dubyak, G. R., Proctor, R. A., and Bertics, P. J. (2001) *J. Immunol.* **167,** 1871–1876
17. Sedgwick, S. G., and Smerdon, S. J. (1999) *Trends Biochem. Sci.* **24,** 311–316
18. Rubstov, A. M., and Lopina, O. D. (2000) *FEBS Lett.* **482,** 1–5
19. Smart, M. L., Gu, B., Panchel, R. G., Wiley, J., Cromer, B., Williams, D. A., and Petrou, S. (2003) *J. Biol. Chem.* **278,** 8853–8860
20. Gu, B. J., Zhang, W. Y., Worthington, R. A., Sluyter, R., Dao-Ung, P., Petrou, S., Barden, J. A., and Wiley, J. S. (2001) *J. Biol. Chem.* **276,** 11135–11142
21. Buell, G., Chessell, I. P., Michel, A. D., Collo, G., Salazzo, M., Herren, S., Gretener, D., Grahames, C., Kaur, R., Kosco-Vilbois, M. H., and Humphrey, P. P. A. (1998) *Blood* **92,** 3521–3528
22. Gu, B. J., Zhang, W. Y., Bendall, L. J., Chessell, I. P., Buell, G. N., and Wiley, J. S. (2000) *Am. J. Physiol.* **279,** C1189–C1197
23. Moore, K. H., Ray, F. R., and Barden, J. A. (2001) *J. Neurosci.* **21,** RC166
24. Slater, M., Murphy, C. R., and Barden, J. A. (2002) *Cell Calcium* **31,** 201–207
25. Wiley, J. S., Chen, R., Wiley, M. J., and Jamieson, G. P. (1992) *Arch. Biochem. Biophys.* **292,** 411–418
26. Sluyter, R., Barden, J. A., and Wiley, J. S. (2001) *Cell Tissue Res.* **304,** 231–236
27. Hickman, S. E., El Khoury, J., Greenberg, S., Schieren, I., and Silverstein, S. C. (1994) *Blood* **84,** 2452–2456
28. Blanpain, C., Wittamer, V., Vanderwinden, J. M., Boom, A., Renneboog, B., Lee, B., Le Poul, E., El Asmar, L., Govaerts, C., Vassart, G., Doms, R. W., and Parmentier, M. (2001) *J. Biol. Chem.* **276,** 23795–23804
29. Bobanovic, L. K., Royle, S. J., and Murrell-Lagnado, R. D. (2002) *J. Neurosci.* **22,** 4814–4824
30. Wiley, J. S., Dao-Ung, L. P., Gu, B. J., Sluyter, R., Shemon, A. N., Li, C., Taper, J., Gallo, J., and Manoharan, A. (2002) *Lancet* **359,** 1114–1119
31. Li, C. M., Campbell, S. J., Kumararatne, D. S., Hill, A. V. S., and Lammas, D. A. (2002) *FEBS Lett.* **531,** 127–131
32. Adriouch, S., Dox, C., Welge, V., Seman, M., Koch-Nolte, F., and Haag, F. (2002) *J. Immunol.* **169,** 4108–4112
33. Jurkat-Rott, K., Lehmann-Horn, F., Elbaz, A., Heine, R., Gregg, R. G., Hogan, K., Powers, P. A., Lapie, P., Vale-Santos, J. E., and Weissenbach, J. (1994) *Hum. Mol. Genet.* **3,** 1415–1419
34. Ophoff, R. A., Terwindt, G. M., Vergouwe, M. N., van Eijk, R., Oefner, P. J., Hoffman, S. M., Lamerdin, J. E., Mohrenweiser, H. W., Bulman, D. E., Ferrari, M., Haan, J., Lindhout, D., van Ommen, G. J., Hofker, M. H., Ferrari, M. D., and Frants, R. R. (1996) *Cell* **87,** 543–552
35. Biervert, C., Schroeder, B. C., Kubisch, C., Berkovic, S. F., Propping, P., Jentsch, T. J., and Steinlein, O. K. (1998) *Science* **279,** 403–406
36. Wallace, R. H., Wang, D. W., Singh, R., Scheffer, I. E., George, A. L., Phillips, H. A., Saar, K., Reis, A., Johnson, E. W., Sutherland, G. R., Berkovic, S. F., and Mulley, J. C. (1998) *Nat. Genet.* **19,** 366–370
37. Lammas, D. A., Stober, C., Harvey, C. J., Kendrick, N., Panchalingam, S., and Kumararatne, D. S. (1997) *Immunity* **7,** 433–444
38. Kusner, D. J., and Adams, J. (2000) *J. Immunol.* **164,** 379–388
39. Fairbairn, I. P., Stober, C. B., Kumararatne, D. S., and Lammas, D. A. (2001) *J. Immunol.* **167,** 3300–3307
40. Solle, M., Labasi, J., Perregaux, D. G., Stam, E., Petrushova, N., Koller, B. H., Griffiths, R. J., and Gabel, C. A. (2001) *J. Biol. Chem.* **276,** 125–132
41. Labasi, J. M., Petrushova, N., Donovan, C., McCurdy, S., Lira, P., Payette, M. M., Brissette, W., Wicks, J. R., Audoly, L., and Gabel, C. A. (2002) *J. Immunol.* **168,** 6436–6445